ISBN: 978-3-95450-232-5 ISSN: 2673-7000 doi:10.18429/JACoW-NAPAC2022-MOPA81

STUDY OF NONLINEAR DYNAMICS IN THE 4-D HÉNON MAP USING THE SQUARE MATRIX METHOD AND ITERATIVE METHODS*

K. Anderson†, Y. Hao, FRIB, Michigan State University, East Lansing, MI, USA
L.-H. Yu, Brookhaven National Laboratory, Upton, NY, USA

Abstract

The Hénon Map represents a linear lattice with a single sextupole kick. This map has been extensively studied due to it's chaotic behavior. The case for the two-dimensional phase space has recently been revisited using ideas from KAM theory to create an iterative process that transforms nonlinear perturbed trajectories into rigid rotations. The convergence of this method relates to the resonance structure and can be used as an indicator of the dynamic aperture. The studies of this method have been extended to the four dimensional phase space case which introduces coupling between the transverse coordinates.

4-D HÉNON MAP

The following is the form of the 4-D area preserving Hénon map:

$$\begin{pmatrix} x \\ p_x \\ y \\ p_y \end{pmatrix}_{n+1} = \begin{pmatrix} \mathbf{R}(\mu_x) & 0 \\ 0 & \mathbf{R}(\mu_y) \end{pmatrix} \begin{pmatrix} x \\ p_x - x^2 + y^2 \\ y \\ p_y + 2xy \end{pmatrix}_n , \tag{1}$$

where $\mathbf{R}(\theta)$ is a clockwise two by two rotation matrix of angle θ, and μ is 2π times the linear tune and whose subscript denotes the dimension. The physical interpretation of this map is a linear one-turn map of a lattice followed by a single thin sextupole kick.

The linear matrix can be diagonalized by using the complex variables $z_x = x - ip_x$ and $z_y = y - ip_y$ which creates the following one turn map:

$$z'_x = \frac{e^{i\mu_x}}{4}\left(-i(z_x^*)^2 - 2iz_x^* z_y + i(z_y^*)^2 + 2iz_y^* z_y - iz_x^2 + 4z_x + iz_x^2\right) \tag{2}$$

$$z'_y = \frac{e^{i\mu_y}}{2}\left(-iz_x^* z_y^* + iz_x^* z_y + iz_y^* z_x + iz_x z_y + 2z_y\right), \tag{3}$$

where the prime denotes the variable after one turn.

In this article, we are expanding a method that transforms the trajectory within the central island to a rigid rotation in a two-dimensional phase space to a four-dimensional phase space.

RIGID ROTATION

Finding a diffeomorphism to a rigid rotation in the 4-D phase space is very analogous to the 2-D derivation [1]. As before we are looking at bounded pseudo-periodic orbits $(z_{x,y}^{(0)}, z_{x,y}^{(1)}, \cdots, z_{x,y}^{(n)}, \cdots)$. KAM theory [2] showed that the invariant tori survive under small nonlinear perturbations and this idea is still applicable to this system so we can expect this diffeomorphism to exist for this case. The significant change is the motion in x and y are coupled so the diffeomorphisms transforming the motion in each θ are not uncoupled and dependent on both rigid rotation angles as this section will show.

As before we express $z_{x,y}$ in terms of a complex phase: $z_{x,y} = e^{i\theta_{x,y}}$. The real part of each θ represents the arguments of z while the imaginary parts relate to the logarithm of the amplitudes of each z. We can then define $f_{x,y}$ as the function of the change in θ after one turn and is dependent on $\theta_x, \theta_x^*, \theta_y, \theta_y^*$ i.e.:

$$\frac{z'_{x,y}}{z_{x,y}} = \exp i(\theta'_{x,y} - \theta_{x,y}) = \exp i f_{x,y}(\theta_x, \theta_x^*, \theta_y, \theta_y^*) . \tag{4}$$

In the case that z_x and z_y are pseudo-periodic we expect θ_x and θ_y to be as well. We can then find diffeomorphisms to a rigid rotation in both θ_x and θ_y:

$$\theta_x = \alpha + h(\alpha, \beta) \tag{5}$$

$$\theta_y = \beta + g(\alpha, \beta) , \tag{6}$$

where h and g are smooth complex functions, which are periodic with respect to α and β and each have a period of 2π. Note that compared to the 2-D phase space, the motion in h and g are coupled and dependent on two angles instead of one. However β and α are still the angles of pure rigid rotations:

$$\alpha_{n+1} = \alpha_n + \rho_x \tag{7}$$

$$\beta_{n+1} = \beta_n + \rho_y , \tag{8}$$

where ρ_x and ρ_y are the rotation numbers:

$$\rho_{x,y} = \lim_{n\to\infty} \frac{\theta_{x,y}^{(n)} - \theta_{x,y}^{(0)}}{n} . \tag{9}$$

Since h and g are periodic it is useful to express them as their Fourier series.

$$h = \sum_{m,n=-\infty}^{\infty} \hat{h}_{n,m} e^{im\alpha + in\beta} \tag{10}$$

$$g = \sum_{m,n=-\infty}^{\infty} \hat{g}_{n,m} e^{im\alpha + in\beta} . \tag{11}$$

From Eq. 4 we use an iterative method to solve for the diffeomorphisms and the rotation numbers starting from

* Work supported by Accelerator Stewardship program under award number DE-SC0019403.
† anderske@frib.msu.edu

Content from this work may be used under the terms of the CC BY 4.0 licence (© 2022). Any distribution of this work must maintain attribution to the author(s), title of the work, publisher, and DOI

ISBN: 978-3-95450-232-5 ISSN: 2673-7000 doi:10.18429/JACoW-NAPAC2022-MOPA81

the initial point ($z_x^{(0)} = x_o - ip_{xo}$, $z_y^{(0)} = y_o - ip_{yo}$). By combining Eq. (4) with Eqs. (5) and (6) we can see how h and g change between turns. The difference between h and g from one turn to the next is f_x and f_y minus the rotation number ρ_x and ρ_y respectively.

We will define f_x and f_y minus their respective rotation numbers as $\eta_x(\rho_x, \alpha, \beta, h(\alpha,\beta), g(\alpha,\beta))$ and $\eta_y(\rho_x, \alpha, \beta, h(\alpha,\beta), g(\alpha,\beta))$.

So for each iteration we solve:

$$h^{(n+1)}(\alpha + \rho_x^{(n+1)}, \beta + \rho_y^{(n+1)}) - h^{(n+1)}(\alpha,\beta) = \eta_x(\rho_x^{(n+1)}, \alpha, \beta, h^{(n)}(\alpha,\beta), g^{(n)}(\alpha,\beta)) \quad (12)$$

$$g^{(n+1)}(\alpha + \rho_x^{(n+1)}, \beta + \rho_y^{(n+1)}) - g^{(n+1)}(\alpha,\beta) = \eta_y(\rho_y^{(n+1)}, \alpha, \beta, h^{(n)}(\alpha,\beta), g^{(n)}(\alpha,\beta)) \,, \quad (13)$$

where the (n) in the superscript denotes iteration number, not turn number. To solve these we use the initial conditions $h^{(0)} = \theta_{xo} - \alpha_0$ and $g^{(0)} = \theta_{yo} - \beta_0$. As with the 2-D case, the zeroth order Fourier components of the left hand side go to zero which gives us the constraint for the rotation numbers. The higher order coefficients will have the form

$$\hat{d}^{(n+1)}(\alpha,\beta) = \frac{\hat{\eta}_{j,nm}^{(n)}}{e^{im\rho_x^{(n+1)} + in\rho_y^{(n+1)}} - 1} \,, \quad (14)$$

where d is h or g and then j will be x or y respectively. Now, the condition condition is visible: The exponential in the denominator cannot equal unity or else that component will go to infinity, and the method will fail to find a solution. These conditions tend to be easier to avoid than in the 2-D case as it requires both rotation numbers to be not ideal.

Lastly, the zeroth order component of h and g ($\hat{h}_{0,0}$ and $\hat{g}_{0,0}$) need to be found. This is done by constraining the diffeomorphism to pass through the initial angles. So for existing α^* and β^* we'll have:

$$\theta_{xo} = \alpha^* + h^{(n+1)}(\alpha^*, \beta^*) \quad (15)$$

$$\theta_{yo} = \beta^* + g^{(n+1)}(\alpha^*, \beta^*) \,. \quad (16)$$

This process will give the rotation numbers and motion of particles in the 4-D phase space.

RESULTS

As we push for larger amplitudes and get closer to the separatrix the method will begin to fail due to η_x and η_y not being smooth enough. In order to remedy this we again utilize the square matrix method (SMM) [3]. Using this method gives us a transformed phase space described by the new complex variables w_x and w_y whose motion compared to z_x and z_y will be closer to a pure rotation and therefore have a more constant amplitude. By truncating the method at some order N and performing a Jordan decomposition on the square matrix to get the generalized eigenvectors we get

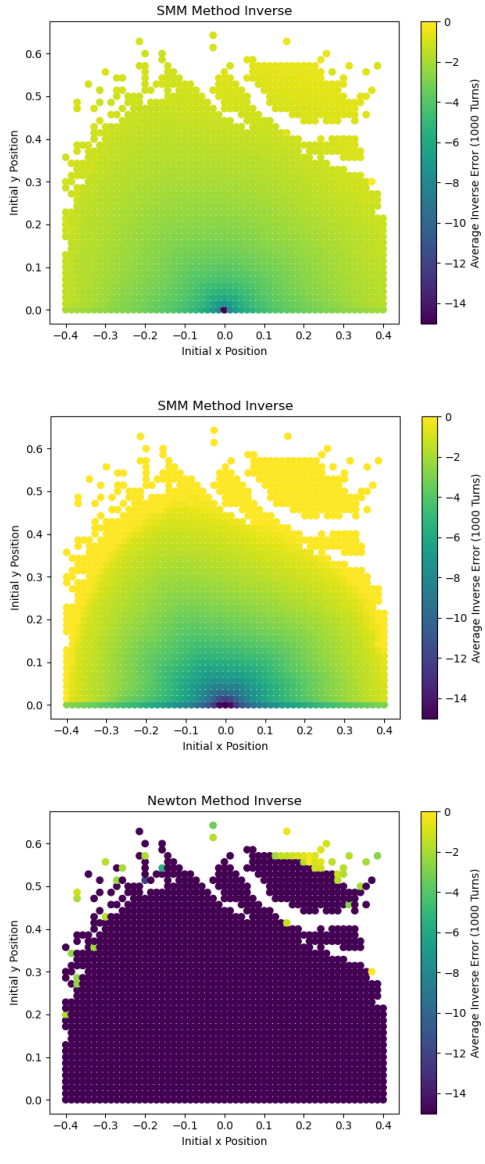

Figure 1: Averaged inverse error for the first 1000 turns using just the 3rd order (a) and 7th order (b) square matrix method and adding Newton's method (c).

the transformations U_x and U_y which describe w_x and w_y in terms of z_x and z_y

$$w_{x,y} = U_{x,y}(z_x, z_y, z_x^*, z_y^*, z_x^2, z_y^2, z_x z_y, \ldots) \quad (17)$$

To return to the original phase space we also need the inverse maps U_x^{-1} and U_y^{-1} which are functions of polynomials of w_x and w_y. These inverses are approximate and accurate up to the calculated order, i.e. $U_{x,y}^{-1} \circ U_{x,y} = I + O\left(z_x^{N+1}, z_y^{N+1}\right)$. To ensure a more accurate inverse in our calculations we perform up to 10 iterations of Newton's method to find z_x and z_y from a given w_x and w_y. The plot (a) and (b) in Fig. 1 show that the inverse of square matrix transformation $U_{x/y}$ can only be determined within an aperture, while the accuracy decreases as the amplitude

Content from this work may be used under the terms of the CC BY 4.0 licence (© 2022). Any distribution of this work must maintain attribution to the author(s), title of the work, publisher, and DOI

ISBN: 978-3-95450-232-5 ISSN: 2673-7000 doi:10.18429/JACoW-NAPAC2022-MOPA81

Content from this work may be used under the terms of the CC BY 4.0 licence (© 2022). Any distribution of this work must maintain attribution to the author(s), title of the work, publisher, and DOI

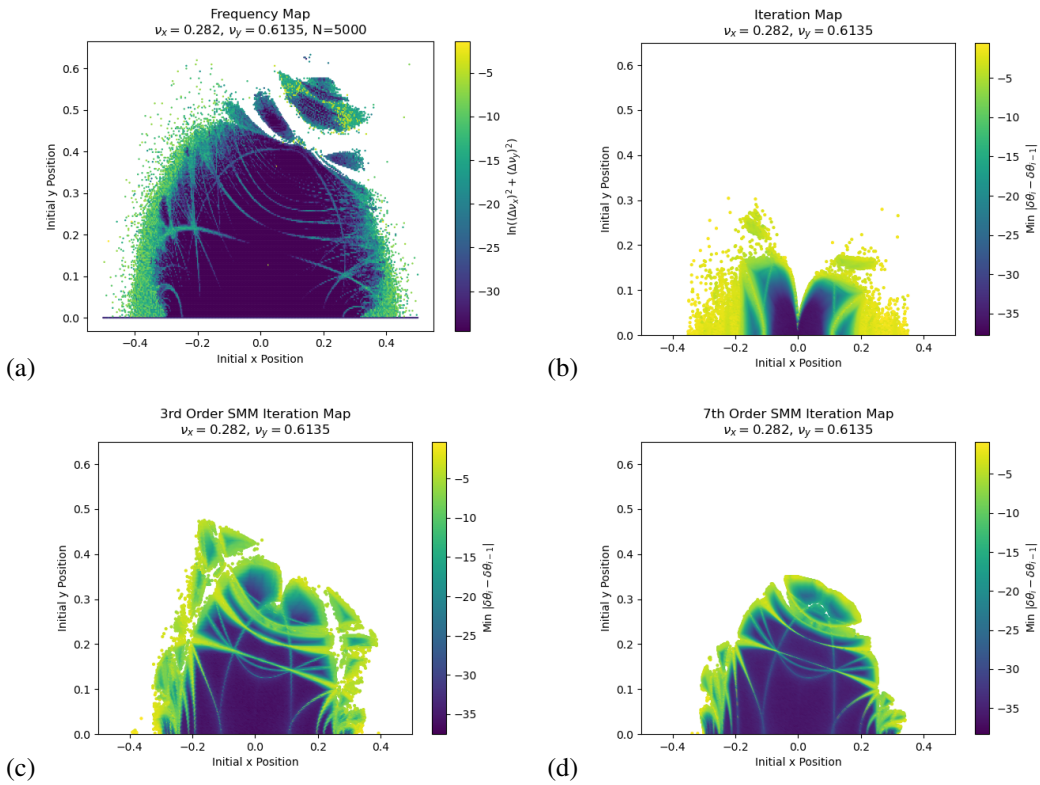

Figure 2: The iteration map for the 4-D transformed Hénon map with linear tunes $\nu_x = 0.282$ and $\nu_y = 0.6153$, using 256 sample points, and w as the variable from the 3rd order (a) and 7th order (b) SMM. The color bar is the minimum difference of $\delta\theta_{x,y}$ between iterations. (c) is the frequency map, the color bar is the natural log of the sum of the squares of the difference in tunes between the first and second halves of each orbit calculated from NAFF.

increases. However, the Newtons' method indeed gives us a more accurate inverse even as we get farther from the origin, as illustrated in Fig. 1 (c). By doing this the inverse only begins to fail near the edge of the aperture. As we will show later, this region is larger than the area of convergence of the iteration method. So we know that the convergence of the iteration method in Fig. 2 is not limited by the accuracy of our inverse function. The same process described in the last section is carried out but with w_x and w_y and their conjugates as our variables for the map. So now $w_{x,y} = e^{i\theta_{x,y}}$ and we can proceed with the method as before.

Figure 2 summarize the dynamic apertures of the 4-D Hénon map with linear tunes $\nu_x = 0.282$ and $\nu_y = 0.6153$, predicted by various methods in the sub-figures. These linear tunes are close to a third order sum resonance $\nu_y = 1 - 2\nu_x$. To evaluate the method proposed in this paper, we can compare it to a frequency map generated with the NAFF algorithm [4], shown in Fig. 2 (a). Comparing with (a), the 2 (b) uses the iteration method directly on the original 4-D Hénon map and only yield a much smaller aperture. Looking at Fig. 2 (b) versus (c) and (d) show that using the SMM extends the area of convergence for our method.

Shown in Fig. 2 (d) is the results of the iterative method being used on the 4-D Hénon map using a 7th order SMM. The indicator used for the colors is the minimum difference of $\delta\theta_{x,y}$ between iterations. If this value is small it suggests that our method is converging on some rotation numbers and orbit. One can see similar features, such as resonance structures, in the iterative map and the frequency map.

One will also notice that the iterative approximation of the dynamic aperture is smaller than ones generated from frequency maps and tracking. We can further extend the range of the aperture from our iteration method by reducing the order of the map used in the SMM to the 3rd order. This is still high enough to resolve the third order resonance but with a lower order there are less terms in the Fourier series of h and g. It is then less likely that one of their coefficients will blow up due to a small denominator from the iteration tunes being close to some resonance. Fig. 2 (c) which uses the 3rd order SMM shows this larger area compared to Fig. 2 (d) which uses the 7th order SMM.

CONCLUSION

We expanded the iteration method used in revisiting the 2-D Hénon Map to be effectively used in the 4-D Hénon Map. The square matrix method plays a critical role in using this iteration method near resonances and expands the area of convergence. Future studies need to be conducted to further push the area of convergence of the iterative method so it can be used as an indicator of the dynamic aperture of a system and so this method can be used in a 6-D phase space.

ISBN: 978-3-95450-232-5 ISSN: 2673-7000 doi:10.18429/JACoW-NAPAC2022-MOPA81

REFERENCES

[1] Y. Hao, K. J. Anderson, and L. H. Yu, "Revisit of Nonlinear Dynamics in Hénon Map Using Square Matrix Method", in *Proc. IPAC'21*, Campinas, SP, Brazil, May 2021, pp. 3788–3791. doi:10.18429/JACoW-IPAC2021-THPAB016

[2] V. Arnold, "Small denominators, 1: Mappings of the circumference onto itself", *AMS Translations*, vol. 46, pp. 213–288, 1965 (Russian original published in 1961).

[3] L. Yu, "Analysis of nonlinear dynamics by square matrix method", *Phys. Rev. Accel. Beams*, vol. 20, no. 3, p. 034001, 2017. doi:10.1103/PhysRevAccelBeams.20.034001

[4] L. Nadolski, J. Laskar, and J. Irwin, "Review of single particle dynamics for third generation light sources through frequency map analysis", *Phys. Rev. ST Accel. Beams*, vol. 6, no. 11, p. 114801, 2003. doi:10.1103/PhysRevSTAB.6.114801.

Content from this work may be used under the terms of the CC BY 4.0 licence (© 2022). Any distribution of this work must maintain attribution to the author(s), title of the work, publisher, and DOI